Colloid Polym Sci (2002) 280: 751–757
DOI 10.1007/s00396-002-0681-4

ORIGINAL CONTRIBUTION

No-Hyung Park
Kyung-Do Suh

The morphology of liquid crystals in monodispersed polymer particles using thermodynamics and diffusion behavior

Received: 6 September 2001
Accepted: 18 November 2001
Published online: 24 April 2002

N.-H. Park · K.-D. Suh (✉)
Division of Chemical Engineering,
College of Engineering,
Hanyang University,
Seoul 133-791, Korea
E-mail: kdsuh@hanyang.ac.kr
Tel.: +82-2-22900526
Fax: +82-2-22952102

Abstract Highly monodisperse poly(methyl methacrylate)/liquid crystal (LC) microcapsules were prepared by a diffusion-controlled polymerization method and were used as a model system for investigating the morphology of the LC domain in the microcapsules. To evaluate the morphology of the microcapsules thermodynamically, the Gibbs free-energy densities of the isotropic, nematic and elastic terms as well as the interfacial tension term were used. As a result, a single LC domain in a microcapsule was favored in equilibrium. The effect of polymerization-induced phase separation on the morphology of the LC domains was also investigated by considering the diffusion behavior of the LCs into the polymer matrix. With proceeding polymerization, the diffusion coefficient of the LCs decreases exponentially. This indicates that a slow polymerization rate favors the formation of a single LC domain by LC diffusion and coalescence.

Keywords Flory–Huggins interaction parameter · Order parameter · Diffusion-controlled polymerization method · Gibbs free-energy density · Interfacial tension

Introduction

Polymer/liquid crystal (LC) composites were the focus of numerous investigations because of their potential applications. Recently, polymer-dispersed LCs (PDLCs) [1, 2, 3, 4, 5, 6] and polymer-stabilized LCs (PSLCs) [7, 8] were intensively investigated and applied in the fields of display devices, owing to some advantages such as being polarizer free, alignment-layer free, the fast response time and simple preparation, etc. Generally, they are fabricated by phase-separation methods [thermally induced phase separation, solvent-evaporation-induced phase separation and polymerization-induced phase separation (PIPS)] [1, 2, 3, 4, 5, 6, 7, 8]. Because the morphology of the LC domains in the polymer matrix depends largely on the conditions during the phase-separation process and affects the electrooptical properties significantly, many researchers have investigated the phase-separation behavior of the LC domains theoretically and experimentally [9, 10, 11, 12, 13, 14, 15, 16, 17]. We previously confirmed that PDLCs from microcapsules showed good electrooptical properties, such as low driving voltage and high sharpness with the electric field.

The phase separation of LCs in polymers depends on the thermodynamics and kinetics of phase separation. It is generally known that LC droplets in PDLCs and PSLCs are formed by the diffusion and coalescence of LCs during the solidification of the polymer matrix. In fast polymerization, small LC domains are observed owing to early freezing of the LC domains that are formed at the beginning of the polymerization. In slow polymerization, large LC domains are formed, owing to the sufficient time for LC diffusion.

In the present study, we prepared monodisperse poly(methyl methacrylate) (PMMA)/LC microcapsules by a diffusion-controlled polymerization method (DPM) [18]. The morphology of the LC domains in the

microcapsules was evaluated by thermodynamics equations considering Flory–Huggins, Maier–Saupe, network and interfacial tension terms, and we also observed the relation between polymerization conversion and the coefficient of diffusion of LCs into the polymer matrix.

Theoretical background

Onsager [9], Flory–Huggins and Maier–Saupe developed several statistical theories about anisotropic phases. Maier-Saupe [10, 11] introduced the concept of nematic order parameter, s, and Flory and Ronca [12, 13] extended the original lattice model to include anisotropic terms [14, 15, 16, 17] and used it to include the phase behavior of the polymer/LC system. Thermodynamics consideration of phase equilibrium can be described by evaluating the Gibbs free-energy density, g [19]. Phase mixing occurred for $g<0$, and phase separation is observed for $g>0$.

$$g = g^{\mathrm{i}} + g^{\mathrm{n}} + g^{\mathrm{e}} + g^{\mathrm{t}}, \tag{1}$$

where g is defined as the algebraic sum of isotropic, g^{i}, nematic, g^{n}, elastic, g^{e}, and interfacial tension, g^{t}, terms. On the basis of Flory–Huggins lattice theory [20] g^{i} can be illustrated by the following equation:

$$g^{\mathrm{i}} = \frac{\Delta G^{\mathrm{i}}}{nkT} = \frac{\phi_{\mathrm{L}} \ln \phi_{\mathrm{L}}}{r_{\mathrm{L}}} + \chi \phi_{\mathrm{L}} \phi_{\mathrm{P}}, \tag{2}$$

where ΔG^{i} is Gibbs free energy,.n, k, and T are the number of moles of the component, the Boltzmann constant, and the absolute temperature. ϕ_{L}, ϕ_{P}, and r_{L} are the volume fraction of LC and polymer ($\phi_{\mathrm{P}} + \phi_{\mathrm{L}} = 1$) and the number of lattice sites occupied by the LC molecules. χ is the Flory–Huggins interaction parameter. It can be obtained from the solubility parameter, δ, which is calculated using group contribution theory [21, 22]:

$$\delta = \frac{\sum \delta_i X_i}{\sum X_i}, \tag{3}$$

where δ_i and X_i are the solubility parameter and the volume fraction of the ith component. χ is calculated using Eq. (4):

$$\chi \approx -0.34 + \frac{(\delta_{\mathrm{p}} - \delta_{\mathrm{s}})^2 V}{RT}, \tag{4}$$

where δ_{p} and δ_{s} are the solubility parameters of polymer and solvent. R and V are the gas constant and the molar volume of the solvent.

For the anisotropic LC, a concept can be developed following Maier–Saupe [23]:

$$g^{\mathrm{n}} = \frac{1}{r_{\mathrm{L}}} \left(-\phi_{\mathrm{L}} \ln z + \frac{1}{2} v \phi_{\mathrm{L}}^2 s^2 \right). \tag{5}$$

The normalized partition function, z, and s are defined by the integrals

$$z = \int_0^1 \exp\left(\frac{3}{2} m x^2 - \frac{1}{2} m \right) dx \tag{6}$$

and

$$s = \frac{3}{2} \frac{\int_0^1 x^2 \exp\left(\frac{3}{2} m x^2 - \frac{1}{2} m\right) dx}{\int_0^1 \exp\left(\frac{3}{2} m x^2 - \frac{1}{2} m\right) dx} - \frac{1}{2}, \tag{7}$$

where $x = \cos\theta$ and θ is the angle between the LC directors and the z-axis. The quantity m, a mean-field parameter characterizing the strength of the orientational potential field of LC directors, and v, the Maier–Saupe interaction parameter, are described by

$$m = v \phi_{\mathrm{L}} s \tag{8}$$

and

$$v = 4.541 \frac{T_{\mathrm{NI}}}{T}. \tag{9}$$

For flexible isotropic polymeric networks g^{e} is assumed for ideal Gaussian chains and is given by

$$g^{\mathrm{e}} = \left(\frac{3\alpha_{\mathrm{e}}}{2r_{\mathrm{c}}} \right) \Phi_0^{2/3} \left(\phi_{\mathrm{P}}^{1/3} - \phi_{\mathrm{P}} \right) + \left(\frac{\beta_{\mathrm{e}}}{r_{\mathrm{c}}} \right) \phi_{\mathrm{P}} \ln \phi_{\mathrm{P}}, \tag{10}$$

where r_{c} is the segment length between cross-links. Φ_0 represents the volume fraction of the network in the bulk polymer. The network parameters α_{e} and β_{e} are 1 and 2/(functionality) in the affine network model [24] and 1 and 0 in the phantom network model [25], respectively.

In our system, it is expected that phase separation between polymer and LC is affected by interfacial tension, owing to the interaction between the LC and the outer aqueous phase in the PIPS process. g^{t} can be expressed as [26]

$$g^{\mathrm{t}} = \frac{1}{RT} \left(\sum \gamma_{ij} A_{ij} - \gamma_0 A_0 \right), \tag{11}$$

where γ_{ij} is the interfacial tension between i and j. A_{ij} is the corresponding interfacial area. γ_0 and A_0 are the interfacial tension and the interfacial area of the original polymer.

Experimental

Materials

Methyl methacrylate (MMA, Junsei Chemicals), methanol (Mallinckrodt Co.), Aerosol OT (Sigma Chemicals), azobis(isobutyronitrile) (Junsei Chemicals), poly(vinyl pyrrolidone) (M_w = 40,000 $gmol^{-1}$, Sigma Chemicals), styrene (St, Junsei Chemicals), poly(propylene glycol) diacrylate (PPG-DA), sodium dodecyl sulfate (SDS, Yakuri Chemicals), ethanol (99.95%, Baker Co.), distilled deionized (DDI) water, benzoyl peroxide (BPO, Junsei Chemicals), sodium nitrite (Junsei Chemicals), and poly(vinylalcohol) (PVA, $M_w = 8.8\times10^4$–9.2×10^4 $gmol^{-1}$) were used without further purification. Low-molecular-weight liquid crystal E7 (T_{NI} = 61 °C), composed of cyanobiphenyls and cyanoterphenyls, was purchased from Merck Co.

Preparation of PMMA/LC microcapsules

MMA was polymerized at 55 °C for 24 h with 50-rpm stirring by dispersion polymerization. Encapsulation was performed by swelling the PMMA seed particles with the LC, cross-linker, and the monomer mixture using a DPM [18]. Firstly, PMMA seed particles were dispersed in 40 g of a solution of ethanol and 0.25 wt% SDS aqueous solution in a 1:4 ratio (SE solution) via sonication and mechanical stirring. A homogeneous mixture of MMA, St, PPG-DA, E7, and BPO was emulsified in 15 g SE solution using a homogenizer at 20,000 rpm for 5 min with sonication. The predispersed PMMA particles were swollen with the mixed emulsion at room temperature with 200-rpm stirring via the Ostwald ripening mechanism. The DPM process was continued until the emulsion disappeared completely. Then, 10 g 5 wt% PVA solution and 50 g 0.2 wt% $NaNO_2$ solution were added slowly and the swollen particles were polymerized at 55 °C for 7 h. After this procedure, monodisperse polymer/LC microcapsules were incorporated into mononuclear LC droplets, owing to PIPS. Then, the microcapsules were washed with repeatedly water and dried at room temperature. A standard recipe for PMMA seed preparation and the DPM process is shown in Tables 1 and 2. The schematic representation of PMMA/E7 microcapsule preparation is described in Scheme 1.

Morphology investigation

The diffusion behavior of the LCs in the polymer was investigated by employing a contact method [26, 27, 28]. A homogeneous mixture of PMMA, St, MMA, PPG-DA, and BPO was placed between a glass and a KBr plate and was polymerized at 60 °C for various times [18]. The LC was injected into the glass–KBr cell to form a LC/polymer interface. The cells were placed in a convection oven at 50 °C for 1 day to diffuse E7 into the polymer matrix. The diffusion behavior of E7 was measured by monitoring the characteristic peak of E7 (around 2,250 cm^{-1}) with IR microscopy (Nicolet Magna IR 760).

Table 1 A standard recipe for the preparation of poly(methyl methacrylate) (*PMMA*) seed particles. 55 °C, 24 h; 10 wt% of monomer concentration based on total weight

Ingredients	Weight (g)
Methyl methacrylate	10
Poly(vinyl pyrrolidone)[a]	4
Aerosol OT	0.45
Azobis(isobutyronitrile)[b]	0.1
Methanol	85.45

[a]4 wt% of poly(vinyl pyrrolidone) (M_w = 40,000 $gmol^{-1}$) based on total weight
[b]1 wt% of azobis(isobutyronitrile) based on monomer weight

Table 2 The recipe for the preparation of PMMA/liquid crystal microcapsules

Ingredients	PLM1	PLM2	PLM3
Seed dispersion process			
PMMA seed		0.5	
SE solution[a]		40	
Diffusion-controlled polymerization process			
1. Swelling stage			
MMA	0.4	0.4	0.4
Styrene	0.29	0.29	0.29
Poly(propylene glycol) diacrylate[b]	0.003	0.003	0.003
E7	0.3	0.5	0.75
Benzoyl peroxide	0.007	0.007	0.007
SE solution[a]	15	15	15
2. Polymerization stage			
$NaNO_2$ solution[c]		50	
Poly(vinyl alcohol) solution[d]		10	

[a]Ethanol:0.25 wt% sodium dodecyl sulfate aqueous solution = 1:4
[b]Poly(propylene glycol) diacrylate as a cross-linker was synthesized and characterized in our previous work [18]
[c]0.2 wt% $NaNO_2$ aqueous solution
[d]5 wt% PVA aqueous solution

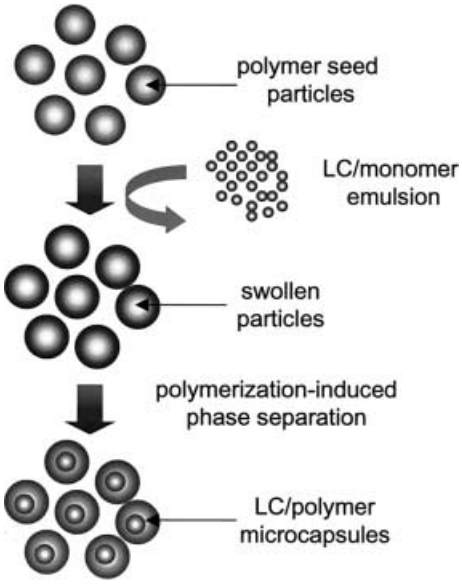

Scheme 1. Representation of the diffusion-controlled polymerization process

Measurements and numerical calculation

The morphology of the PMMA seed particles and the PMMA/E7 microcapsules were determined with a scanning electron microscope (Hitachi), an optical microscope (Olympus BH-2), and a polarized optical microscope (POM, Olympus BH-2) equipped

with an image analyzer. Numerical calculation was carried out using Mathematica version 3.0 and Borland C^{++} version 3.0 with an IBM-compatible computer.

Results and discussion

Monodisperse PMMA/E7 microcapsules [18] having monosized LC domains were used as a model system for describing the phase behavior and the morphology of the LC domains in the microcapsules. It is supposed that the morphology of the LC domains in the microcapsules depends on the interfacial tension, the diffusion, and the coalescence of the LCs in the polymer matrix.

The morphology of the PMMA seed particles and the PMMA/E7 microcapsules is illustrated in Fig. 1. The PMMA seed particles showed high monodispersity and spherical shape. Their number-average size, R_n, and polydispersity (PDI) were 3.772 μm and 1.003. Their monodispersity and shape ($R_n = 4.58$ μm, PDI = 1.007) were maintained even after the LC had been encapsulated in the polymer particles. The phase-separated LC domains in the microcapsules were observed with a POM (Fig. 2).

A single E7 domain in a microcapsule was formed and showed monodispersity. The size of the LC domains in the microcapsules increased with increasing LC content (PLM1 < PLM2 < PLM3). Thus, the LC droplet size can be controlled by the amount of LC introduced in some range, and the formation of a single LC domain is favored. Our system can be considered as an ideal system for evaluating the phase behavior.

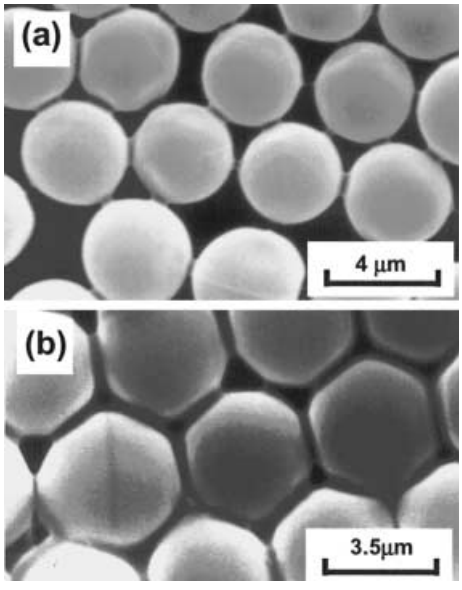

Fig. 1 The morphology of E7 microcapsules as observed by scanning electron microscopy: **a** poly(methyl methacrylate) (*PMMA*) seed particles; **b** liquid crystal (*LC*) microcapsules (PLM3)

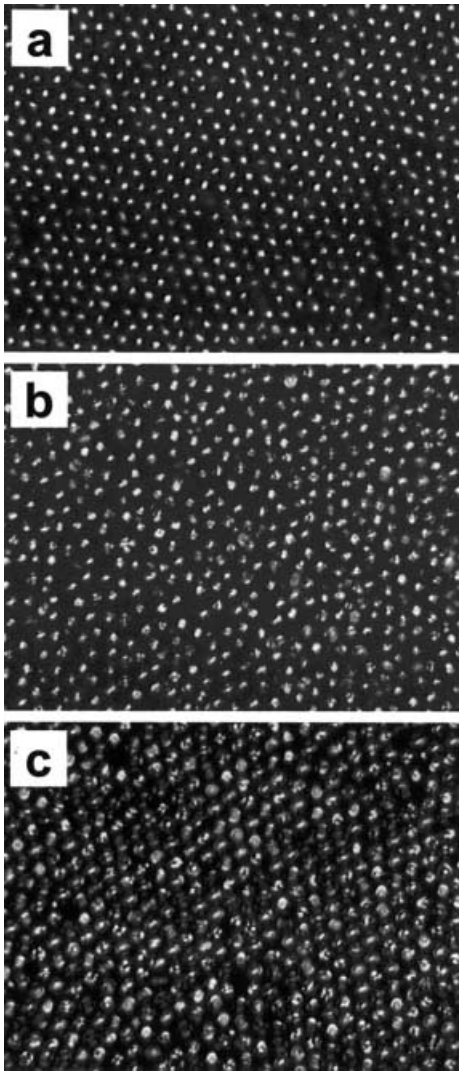

Fig. 2 The morphology of E7 microcapsules observed with a polarized optical microscope (*POM*): **a** PLM1; **b** PLM2; **c** PLM3

The phase behavior of conventional PDLC systems composed of bulk polymer and LC is described by g^i, g^n, and g^e only; however, in our system, g^t is expected to affect the phase behavior and morphology of the LC domain in the microcapsules, since complete phase separation occurs in the aqueous phase. To calculate g^i (Eq. 2), r_L was assumed to be 1. The interaction parameters of 0.775, 0.821, and 0.847 for PLM1, PLM2, and PLM3 at 30 °C were calculated.

The relationship between m and s, calculated with Eqs. (6), (7), and (8) is illustrated in Fig. 3a. The relationship between s and T was calculated from Fig. 3a. The critical order parameter $s_c = 0.443$ and $T_{NI} = 334$ K were obtained on the basis of Fig. 3a.

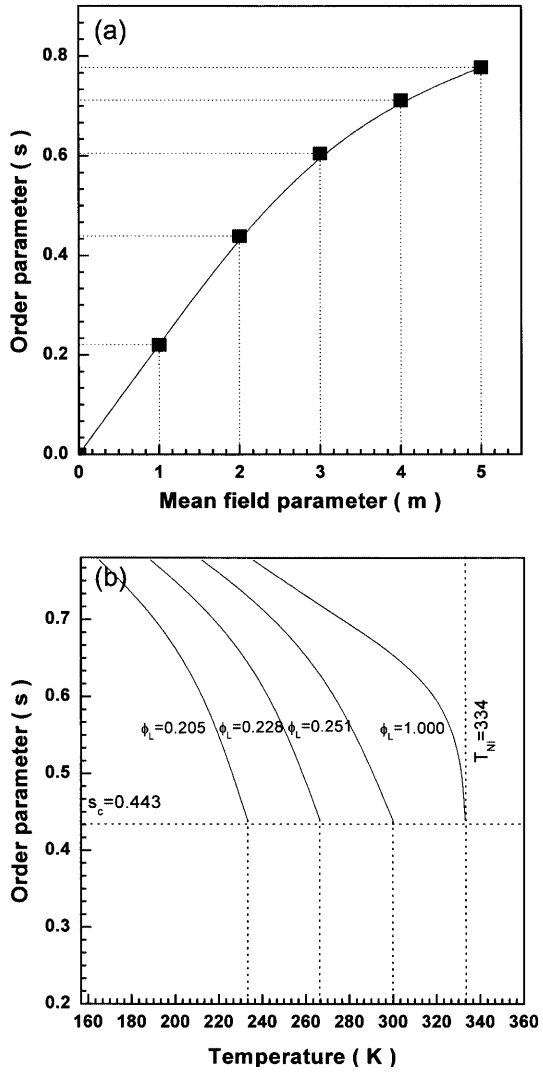

Fig. 3 Change in the order parameter, s, with **a** the mean field parameter, m, and **b** the temperature for different volume fractions of the LC, ϕ_L

We obtained s for E7 in the polymer as a function of T and ϕ_L. It increases with m and decreasing T. At s_c, s drops sharply to zero, indicative of a first-order transition. It is important to note that the phase behavior is unaffected by cross-linking. This enables s to be applied for both linear and cross-linked polymers. For the calculation of g^e, Φ_0 was assumed to be equal to ϕ_P during polymerization and our network system behaves like a phantom network model. For the calculation of g^t, interfacial tension terms between the polymer and water, between the LCs and water, and between the polymer and water were considered. We removed the LC–water term because the E7 domain is not in contact with the water phase as confirmed by the POM measurements, and the polymer–water term is assumed to be constant. With these two assumptions, we simplify g^t to the following equation:

$$g^t = \frac{1}{RT}\left(\gamma_{PW}A_{PW} + \gamma_{PL}A_{PL}\sqrt[3]{x}\right), \tag{12}$$

where x is the number of LC domains in a microcapsule. The morphology of the number of phase-separated LC domains in a microcapsule was predicted from thermodynamics (Fig. 4).

The value of g increases with x, owing to the increase in the interfacial area between the LC domain and the polymer matrix. This means that the system becomes unstable with increasing x, resulting in a single LC domain in a microcapsule in the equilibrium state.

A single LC domain in a microcapsule is of course thermodynamically stable; however, it is well known that the morphology of polymer/LC composites is also affected significantly by the diffusion and coalescence of the LCs in the polymer matrix. Thus, the LC diffusion rate during polymerization must also be considered. Because it is impossible to investigate the diffusion behavior of the LCs in the polymer particles during the polymerization, the investigation of LC diffusion was carried out in the bulk polymer via the contact method [26, 27, 28] using IR microscopy. Polarized optical microscopy results of the polymer/LC contact cell and the results of IR microscopy measurements are shown in Fig. 5.

After 1 day, we observed a broadened LC domain in the bulk polymer phase. The degree of diffusion was characterized by monitoring the absorption peak at 2,250 cm^{-1} (–CN peak) and the ratio of the absorbance intensity for diffused LC to that for pure LC (A/A_0). These results are summarized in Fig. 6.

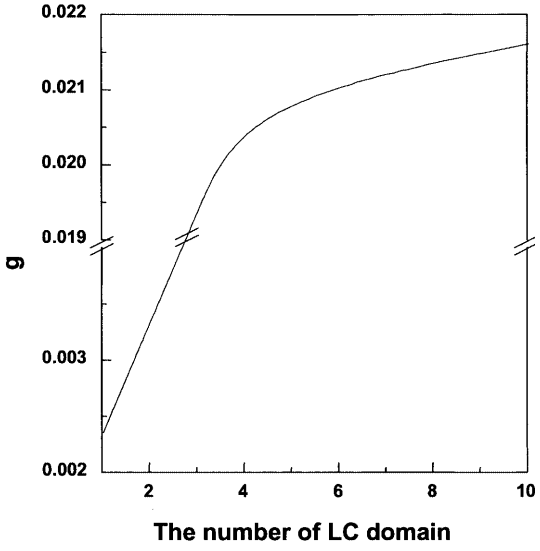

Fig. 4 Increase in the Gibbs free-energy density, g, with the number of LC domains in a microcapsule (PLM3)

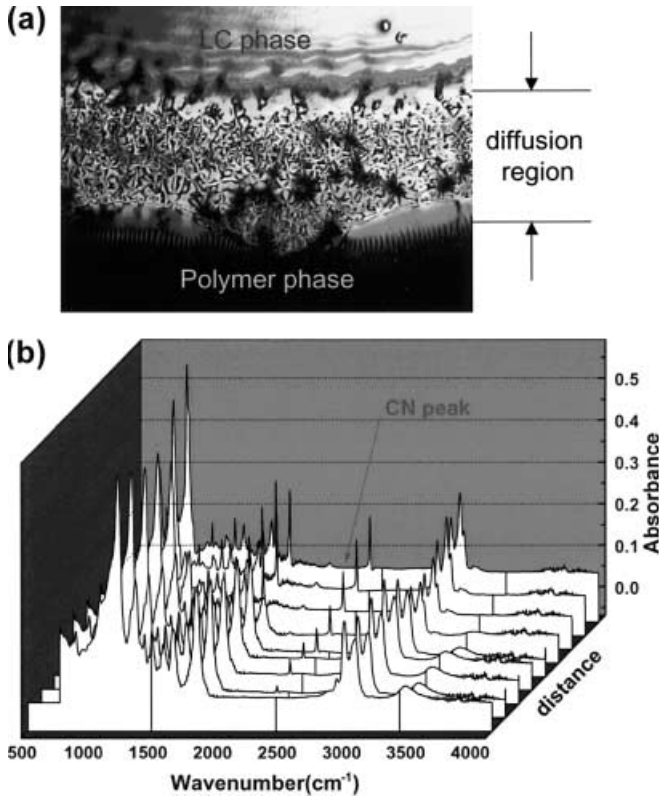

Fig. 5 Contact method for investigation of LC diffusion: **a** POM photographs of the polymer and the E7 contact cell; **b** IR spectra as a function of distance

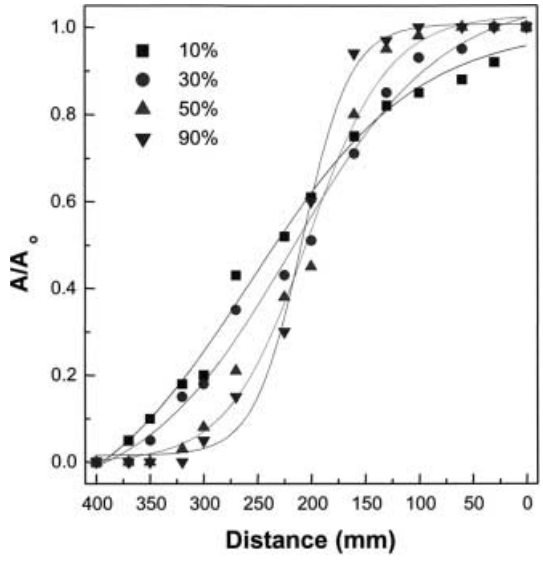

Fig. 6 The diffusion of the LC in the polymer matrix at different polymerization rates

During the polymerization, the diffusion decreases. At high polymerization conversion, A/A_0 is large near the polymer/LC interface and decreases significantly away from the interface. Generally, the diffusion of low-molecular-weight LCs into a polymer phase obeys Fick's second law, and the results can be fitted by

$$\frac{A}{A_0} = \mathrm{erf}\left(\frac{d}{2\sqrt{Dt}}\right), \tag{13}$$

where

$$\mathrm{erf}x = \frac{2}{\sqrt{\pi}\int_0^x \exp(t^2)\mathrm{d}t}. \tag{14}$$

and where D and t are the diffusion coefficient and time. d is the distance from the polymer/LC interface. Indeed, our system follows Fick's second law. We calculated D by using the earlier equations (Table 3, Fig. 7).

D decreases significantly as the polymerization conversion, C, increases. The change with C can be described by and plotted using the following equation:

$$D(C) = 5.25 \times 10^4 \exp\left(-\frac{C}{12.18}\right), \tag{15}$$

where $D(C)$ is a polymerization-dependent diffusion coefficient which decays exponentially.

During polymerization, the viscosity of the polymer matrix also increases, and the LC diffusion rate

Table 3 The diffusion coefficient with polymerization conversion

Polymerization conversion (%)	Diffusion coefficient (cm^2/s)
10	2.31×10^{-4}
30	4.78×10^{-5}
50	8.80×10^{-7}
90	1.32×10^{-7}

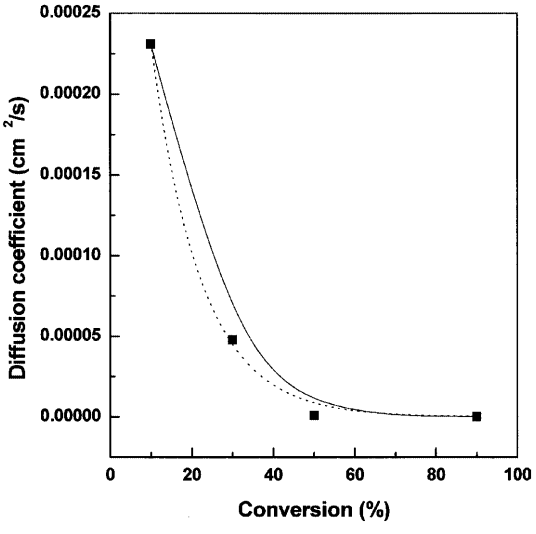

Fig. 7 Change in the diffusion coefficient with the polymerization conversion: curve fitting, *solid line*; experiment, *dotted line*

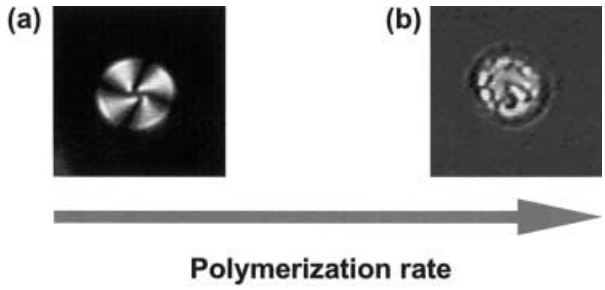

Fig. 8 POM observation with increasing polymerization rate: **a** polymerization in our system (slow polymerization); **b** UV curing (fast polymerization)

decreases drastically. Finally, LC droplets no longer diffuse when polymerization was complete. This morphology of the LC domain can be controlled by the polymerization rate. During the slow polymerization, the diffusion and coalescence of the LCs are important. Therefore, the possibility for the formation of a single LC domain in a microcapsule increases. In contrast, many small LC domains in a microcapsule are observed in the case of fast polymerization. The results are confirmed by the POM observation (Fig. 8).

Conclusions

Monosized LC microcapsules were prepared by a DPM. The morphology of phase-separated LC domains was described using the algebraic sum of g^{i}, g^{n}, g^{e}, and g^{t}. A single LC domain in a microcapsule is thermodynamically favored. The LC diffusion in the polymer matrix was also investigated during the polymerization by a contact method. As the degree of polymerization increased, D decreased exponentially. When the LC diffusion in the polymer matrix is low, LC multidomains are formed; however, in the case of the slow polymerization in our system, diffusion was fast enough to create single LC domains which were stable in a thermodynamic sense.

Acknowledgement This work was supported by the Brain Korea 21 Project.

References

1. Craighead HG, Cheng J, Hackwood S (1982) Appl Phys Lett 40:22
2. Kawatsuki N, Ono H (1995) J Appl Polym Sci 55:911
3. Shimada E, Uchida T (1992) Jpn J Appl Phys 31:352
4. Doane JW, Golemme A, West JL, Whitehead JR, Wu BG (1988) Mol Cryst Liq Cryst 65:511
5. Pane S, Caporusso M, Hakemi H (1997) Liq Cryst 23:861
6. Chien LC, Lin C, Fredley DS, McCargar JW (1992) Macromolecules 25:133
7. Rajaram CV, Hudson SD, Chien LC (1995) Chem Mater 7:2300
8. Rajaram CV, Hudson SD, Chien LC (1996) Chem Mater 8:2451
9. Onsager L (1949) Ann NY Acad Sci 51:627
10. Maier W, Saupe A (1959) Z Naturforsch A 14:882
11. Maier W, Saupe A (1960) Z Naturforsch A 15:287
12. Flory PJ, Ronca G (1979) Mol Cryst Liq Cryst 54:311
13. Flory PJ, Ronca G (1979) Mol Cryst Liq Cryst 54:289
14. Motoyama M, Nakazawa H, Ohta T, Fujisawa T, Nakada H, Hayashi M, Aizawa M (2000) Comput Theor Polym Sci 10:287
15. Benmouna F, Daoudi A, Roussel, Busine JM, Coquert X, Maschke U (1999) J Polym Sci Part B Polym Phys 37:1841
16. Nwabunma D, Kyu T (1999) Macromolecules 32:664
17. Nwabunma D, Chiu HW, Kyu T (2000) Macromolecules 33:1416
18. Park NH, Park SI, Suh KD (2001) Colloid Polym Sci 279:1082
19. Shen C, Kyu T (1995) J Chem Phys 102:556
20. Ballauff M (1986) Mol Cryst Liq Cryst 4:15
21. Krevelen V (1990) Properties of polymers, 3rd edn. Elsevier, Amsterdam
22. Lin HM, Nash RA (1993) J Pharm Sci 82:1018
23. Chiu HW, Kyu T (1995) J Chem Phys 103:7471
24. Flory PJ (1950) J Chem Phys 18:108
25. James H, Guth EJ (1947) J Chem Phys 15:669
26. Challa SR, Wang SQ, Koenig JL (1995) Appl Spectrosc 49:267
27. Challa SR, Wang SQ, Koenig JL (1997) Appl Spectrosc 51:297
28. Mcfarland CA, Koenig JL, West JL (1993) Appl Spectrosc 47:321